JOURNAL OF GEOPHYSICAL RESEARCH, VOL. 93, NO. D6, PAGES 7047–7054, JUNE 20, 1988

Infrared Radiation Models for Atmospheric Ozone

DAVID P. KRATZ[1] AND ROBERT D. CESS

Institute for Atmospheric Sciences, State University of New York at Stony Brook

A hierarchy of line-by-line, narrow-band and broadband infrared radiation models are discussed for ozone, a radiatively important atmospheric trace gas. It is shown that the narrow-band (Malkmus) model is in near-precise agreement with the line-by-line model, thus providing a means of testing narrow-band Curtis-Godson scaling, and it is found that this scaling procedure leads to errors in atmospheric fluxes of up to 10%. Moreover, this is a direct consequence of the altitude dependence of the ozone mixing ratio. Somewhat greater flux errors arise with use of the broadband model, due to both a lesser accuracy of the broadband scaling procedure and to inherent errors within the broadband model, despite the fact that this model has been tuned to the line-by-line model.

1. INTRODUCTION

It is well known that ozone exerts a significant impact upon the Earth's surface-atmosphere energy budget. With absorption features in both the solar and infrared portions of the spectrum, ozone plays a very complicated role, influencing the climate through both radiative and dynamical interactions between the stratosphere and troposphere [*Ramanathan and Dickinson*, 1979]. This emphasizes the need to have accurate radiative transfer models for this gas. Toward this goal, one purpose of the present study is to develop mutually consistent line-by-line, narrow-band and broadband infrared radiation models for the 9.6- and 14-μm bands of ozone. A second goal is to employ ozone as an illustrative gas for the purpose of appraising the applicability of scaling approximations when the gas mixing ratio varies significantly with altitude, as is the case with ozone. This second goal is motivated by suggested errors inherent within Curtis-Godson scaling when applied to atmospheric ozone [e.g., *Rodgers and Walshaw*, 1966; *Yamamoto et al.*, 1972; *Kuriyan et al.*, 1977].

The overall strategy closely follows a related study by *Cess et al.* [1986] pertaining to atmospheric methane. We begin with a discussion of the reference line-by-line calculation, and we then show that the Malkmus narrow-band model yields band absorptances which are very comparable to those of the line-by-line model. Next, a broadband model is tuned, for a homogeneous gas, to the line-by-line model, in such a manner that a hierarchy of band models is obtained which yields comparable homogeneous band absorptances. With reference to the line-by-line model, this then affords a means of appraising the accuracy of scaling approximations for both the narrow-band and broadband models when they are applied to atmospheric radiation calculations. Finally, an intercomparison of the various models is presented for both flux and heating rate calculations. Differences between the models are noted as well as the differences incurred through employing either a Voigt or Lorentz line shape.

2. RADIATION MODELS

Line-by-Line Model

The line-by-line calculations incorporate both Voigt and Lorentz line shapes, a wave number integration interval of 10^{-2} cm^{-1}, and a wave number cutoff of 5 cm^{-1}; i.e., the spectral absorption coefficient includes the effects of all rotational lines within a 10 cm^{-1} range, centered at the wave number of the absorption coefficient calculation. Both the integration interval and the cutoff were chosen on the basis of sensitivity studies.

The line locations, intensities, and lower-state energies were taken from the 1982 version of the AFGL data tape [*Rothman et al.*, 1983], incorporating all O_3 lines within the wave number interval 945–1250 cm^{-1} for the 9.6-μm band. The temperature dependence of the line intensities, $S(T)$, is given by

$$S(T) = S_0\left(\frac{T_0}{T}\right)^{3/2} \exp\left[\frac{hc}{k}E''\left(\frac{1}{T_0}-\frac{1}{T}\right)\right] \quad (1)$$

where h is Planck's constant, c is the speed of light, k is Boltzmann's constant, E'' is the energy of the lower state, $T_0 = 296$ K, and S_0 is the line intensity, in units of (cm^2 atm)$^{-1}$, at T_0. The air-broadened Lorentz half width per unit pressure, γ^0, was taken to be

$$\gamma^0(\text{cm}^{-1}\ \text{atm}^{-1}) = \gamma^0(T_0/T)^{0.72} \quad (2)$$

for all lines, where γ^0 is the half width for the entire band, with $\gamma^0 = 0.083$ for the 9.6-μm band and $\gamma^0 = 0.077$ for the 14-μm band. The exponent for the temperature dependence is adopted from *Aida* [1975], and *Ramanathan and Dickinson* [1979].

Our choice of $\gamma^0 = 0.083$ for all lines within the 9.6-μm band is at minor variance with the AFGL tape, which contains some half widths that depart from this single value. We have, however, also incorporated the AFGL values for γ^0 within the line-by-line calculation, and we find that use of the single 0.083 value produces the negligible error of 0.003%.

On a further point, our inclusion of the 14-μm O_3 band is solely motivated by the incorporation of this band within the World Meteorological Organization report on intercomparison of radiation codes in climate models (ICRCCM) [*Luther and Fouquart*, 1984]. For atmospheric applications the importance of this band is minimal because of overlap by the strong 15-μm CO_2 band.

[1]Now at NASA Goddard Space Flight Center, Greenbelt, Maryland.

Paper number 8D0218.
0148-0227/88/008D-0218$05.00

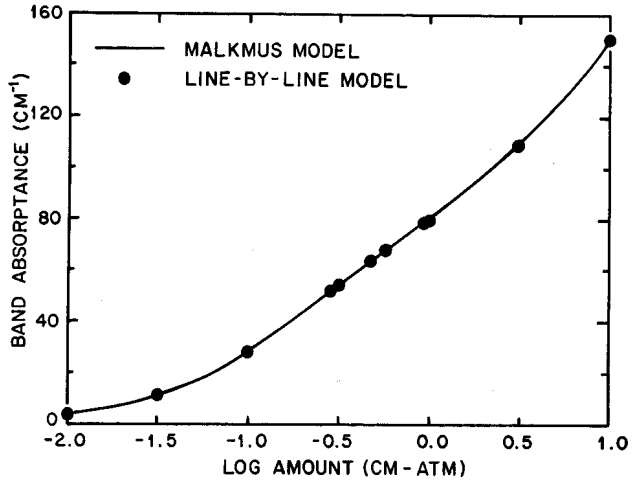

Fig. 1. Band absorptance comparison for the 9.6-μm ozone band. The ozone amount refers to standard temperature.

Narrow-Band Model

The two most widely used narrow-band (or random-band) models are those of *Goody* [1952] and *Malkmus* [1967]. As discussed by *Cess et al.* [1986], neither model produces satisfactory agreement with line-by-line calculations for the 7.6-μm band of methane. Instead, they found that a modified version of the Goody model, incorpoating a correction for coincident and near-coincident lines, proved to be very satisfactory. But *Cess et al.* [1986] emphasized that such conclusions were dependent upon the specific gas under consideration. Indeed, as will be illustrated shortly, the situation is quite different for ozone.

Specifically, it will be shown that the Malkmus model constitutes a very adequate narrow-band model for O_3. Letting $T_{\Delta\omega}$ denote the transmittance for a given spectral interval $\Delta\omega$, the *Malkmus* [1967] model is given by

$$T_{\Delta\omega} = \exp\left\{-\frac{\pi\bar{\gamma}}{2\Delta\omega}\left[\left(1+\frac{4S_{\Delta\omega}m}{\pi\bar{\gamma}}\right)^{1/2}-1\right]\right\} \qquad (3)$$

where $S_{\Delta\omega}$ is the sum of the line intensities within the interval $\Delta\omega$, m is the absorber amount, and $\bar{\gamma}$ is defined by the relation

$$\bar{\gamma} = \frac{4}{\pi}\frac{[\sum (S_{JK}\gamma_{JK})^{1/2}]^2}{\sum S_{JK}} \qquad (4)$$

where S_{JK} and γ_{JK} denote the individual line intensities and line half widths, respectively, and the summation is over all lines with $\Delta\omega$.

The spectroscopic data employed in the narrow-band models are identical to those used in the line-by-line calculation. For present purposes the narrow-band computations were carried out with $\Delta\omega = 5$ cm^{-1}. As discussed by *Kiehl and Ramanathan* [1983] with respect to atmospheric CO_2, significant errors can occur if one employs overly large spectral intervals. This is due to the statistics of the band structure, as manifested by the averaging procedure of (4), being variable throughout the band. The use of narrow intervals will of course minimize this effect, but if the interval is too narrow, it will not contain a sufficient number of lines to yield meaningful statistics.

Ideally, there should exist an interval range over which the computed band absorptance is nearly invariant to the size of the interval. As demonstrated by *Cess et al.* [1986], CH_4 does not produce such a clearly defined range of intervals. We presently find, however, that O_3 is much better behaved. For a temperature of 263 K and a pressure of 0.514 atm, both of which correspond to average values [*Cess et al.*, 1986] for the atmospheric calculations of sections 4 and 5, the absorptance of the 9.6-μm band, as calculated from (3), rises steadily by 7% as the interval width is increased from 2 to 30 cm^{-1}. Thus there would be roughly only a 1% difference in computed band absorptance for $\Delta\omega = 5$ cm^{-1} versus $\Delta\omega = 2$ cm^{-1}. A similar conclusion, utilizing atmospheric flux calculations, has been obtained by *Morcrette and Fouquart* [1985]. For the 14-μm band the $\Delta\omega = 2$–30 cm^{-1} rise is less than 0.5%.

A second potential problem concerns the locations of the wave number intervals; i.e., the choice of the origin. *Cess et al.* [1986] noted that this produces a 5% variation in band absorptance for the 7.6-μm band of CH_4. But for O_3 we find only 0.5 and 0.05% variations for the 9.6- and 14-μm bands, respectively.

Both the Goody and Malkmus narrow-band models have been compared to line-by-line calculations utilizing the previously discussed average atmospheric temperature (263 K) and total pressure (0.514 atm). As for the atmosphere, these

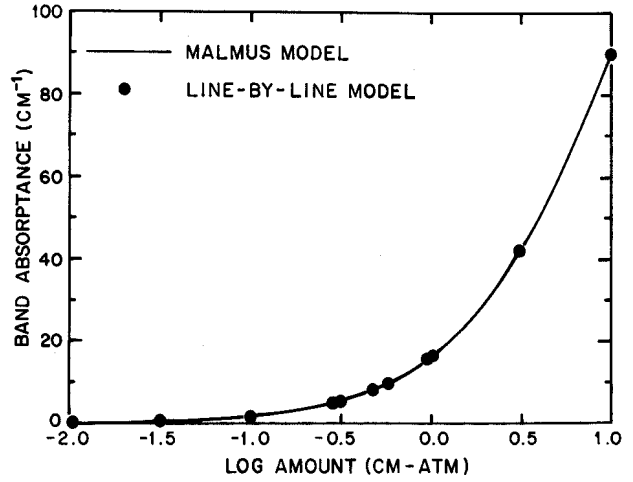

Fig. 2. Band absorptance comparison for the 14-μm ozone band. The ozone amount refers to standard temperature.

TABLE 1. Summary of the 9.6- and 14-μm Ozone Bands

Band	Intensity, cm^{-2} atm^{-1}	Isotope
	9.6 μm	
ν_3	345.871	$^{16}O^{16}O^{16}O$
ν_1	16.647	$^{16}O^{16}O^{16}O$
$\nu_2 + \nu_3 - \nu_3$	11.169	$^{16}O^{16}O^{16}O$
$\nu_3 + \nu_3 - \nu_3$	4.322	$^{16}O^{16}O^{16}O$
$\nu_1 + \nu_3 - \nu_3$	1.529	$^{16}O^{16}O^{16}O$
$\nu_1 + \nu_2 - \nu_1$	0.274	$^{16}O^{16}O^{16}O$
ν_3	1.258	$^{16}O^{16}O^{18}O$
ν_3	0.619	$^{16}O^{18}O^{16}O$
	14 μm	
ν_2	15.586	$^{16}O^{16}O^{16}O$
$\nu_2 + \nu_2 - \nu_2$	1.033	$^{16}O^{16}O^{16}O$

The band intensities refer to 296 K.

TABLE 2. Broadband Parameters for the 9.6- and 14-μm Bands

Parameter	Value
9.6 μm	
A_0, cm^{-1}	$27.93(T/296)^{0.574}$
$\beta_{666}\nu_3$	$11.25P(296/T)^{0.72}$
$\beta_{666}\nu_1$	$6.59P(296/T)^{0.72}$
$\beta_{668}\nu_3$	$5.28P(296/T)^{0.72}$
$\beta_{686}\nu_3$	$4.97P(296/T)^{0.72}$
D	0.733
14 μm	
A_0, cm^{-1}	$65.58(T/296)^{0.602}$
β^{ν_2}	$10.10P(296/T)^{0.72}$
D	0

The subscripts 666, 668, and 686 refer to $^{16}O^{16}O^{16}O$, $^{16}O^{16}O^{18}O$, and $^{16}O^{18}O^{16}O$, respectively.

comparisons refer to trace O_3 abundances, so that air is the broadening gas. For these conditions there is no distinction between use of either the Voigt or Lorentz line shape within the line-by-line calculations, thus assuring consistency with the narrow-band models which incorporate Lorentz line shapes. These comparisons reveal that the Malkmus model produces the best results. Specifically, for a range of O_3 abundances from 0.001 to 10 cm atm, the Goody model overestimates the band absorptance by 2–3% and 3–5% for the 9.6- and 14-μm bands, respectively, whereas the Malkmus model agrees with the line-by-line calculations to within 1% for the 9.6-μm band, while overestimating the 14-μm band absorptance by 1–3%. For this reason, we subsequently adopt the Malkmus narrow-band model. Figures 1 and 2 show comparisons of the Malkmus and line-by-line results, for the 9.6- and 14-μm bands, respectively.

Broadband Model

The broadband model employed here is that given by *Cess et al.* [1986], comprising a hybrid of the models of *Cess and Ramanathan* [1972] and *Ramanathan* [1976]. It is expressed by

$$A = 2A_0 \ln\left\{1 + \sum_i \sum_j \left[\frac{u_{ij}}{D + (E + u_{ij}(1 + 1/\beta_{ij}))^{1/2}}\right]\right\} \quad (5)$$

where $E = (2 - D)^2$, $u_{ij} = S_{ij}m/A_0$, with S_{ij} the band intensity, β is proportional to the ratio of the mean line half width to mean line spacing, and the summations are over isotopes (i) and bands (j).

Table 1 lists the individual bands which make up the 9.6- and 14-μm bands, as compiled on the 1982 version of the AFGL tape [*Rothman et al.*, 1983]. It should be noted that the 9.6-μm band not only incorporates the ν_3 fundamental, but also several ν_3 hot bands, two ν_3 minor isotopic fundamentals, the ν_1 fundamental, and a ν_1 hot band.

The quantities A_0, β_{ij}, and D have been determined through regression fits to line-by-line calculations. These encompass a range of temperatures, pressures, and O_3 abundances appropriate to the Earth's atmosphere. Results for both the 9.6- and 14-μm bands are summarized in Table 2.

For the 14-μm band the fit to the line-by-line calculations was better than 1% for the entire range of temperatures, pressures, and O_3 abundances considered. But for the 9.6-μm band, differences as large as 14% exist, similar to deviations found by *Ramanathan* [1976]. Fortunately, as was also found by Ramanathan, the largest deviations occur when O_3 abundance and total pressure are both large, and these conditions are not representative of atmospheric conditions.

3. Scaling Approximations

This section closely follows the approach of *Cess et al.* [1986], who appraised the applicability of scaling approximations with reference to atmospheric methane. Curtis-Godson scaling constitutes the conventional scaling approximation for use with narrow-band models, and that described by *Rodgers and Walshaw* [1966] is adopted here. With respect to broadband models, there have been three suggested scaling procedures [*Chan and Tien*, 1969; *Cess and Wang*, 1970; *Edwards and Morizumi*, 1970], with Chan-Tien scaling being found by *Cess et al.* [1986] to be the most appropriate. Our present study of atmospheric ozone is consistent with this, and we thus restrict attention solely to Chan-Tien scaling.

To be compatible with *Luther and Fouquart* [1984], we adopt the mid-latitude summer atmosphere of *McClatchey et al.* [1971], a choice which requires some degree of clarification. Recently, it has been pointed out (S. Fels, private communication, 1987) that this model atmosphere contains typographical errors in atmospheric density for altitudes of 25 km and higher and that when corrected the O_3 mixing ratios for these altitudes are reduced by 20–30%. This would have no impact upon an ozone radiation calculation if one utilizes ozone abundances within their radiation code. But the majority of the ICRCCM participants apparently utilized ozone mixing ratios, and there is currently no intent to have these calculations redone (R. Ellingson, private communication, 1987). Thus to be compatible with Luther and Fouquart, we

TABLE 3. Comparison of Tropospheric (0–13 km) O_3 Total Band Absorptances for the 9.6-μm Band

Model	Band Absorptance, cm^{-1}		Ratio	Error, %
	Homogeneous	Nonhomogeneous		
Line-by-line (Voigt)	16.51	16.12	0.976	···
Line-by-line (Lorentz)	16.51	16.12	0.976	···
Narrow band	16.56	16.78	1.013	3.8
Broadband	15.21	14.74	0.969	−0.7

The homogeneous atmosphere (P = 0.587 atm and T = 268 K) contains the same O_3 amount (0.4885 cm atm) as the nonhomogeneous atmosphere. Here as in Tables 4 and 5, the abundance refers to standard temperature, i.e., the units are identical to (cm amagats)$_{STP}$.

TABLE 4. Comparison of Stratospheric (13–50 km) O_3 Total Band Absorptances for the 9.6-μm Band

Model	Band Absorptance, cm^{-1}		Ratio	Error, %
	Homogeneous	Nonhomogeneous		
Line-by-line (Voigt)	39.12	33.63	0.860	···
Line-by-line (Lorentz)	39.05	33.35	0.854	···
Narrow band	39.63	33.43	0.844	−1.9
Broadband	39.18	37.59	0.959	12.3

The homogeneous atmosphere (P = 0.998 atm and T = 259 K) contains the same O_3 amount (0.2454 cm atm) as the nonhomogeneous atmosphere.

initially retain the original (i.e., typographical errors included) *McClatchey et al.* [1971] mid-latitude summer atmosphere and then later present results employing the corrected model atmosphere. Moreover, since we are focusing on the examination of radiative transfer approximations, overlap by water vapor, CO_2, and clouds will be ignored.

To test both the narrow-band (Curtis-Godson) and broadband (Chan-Tien) scaling approximations, we adopt a procedure similar to that employed by *Cess et al.* [1986], which involved comparisons of the total band absorptance for the atmospheric column. But since the O_3 mixing ratio varies strongly with altitude, we first separately consider the column absorptances for the troposphere and stratosphere.

Total band absorptances for the tropospheric column (0–13 km), as determined employing the line-by-line calculation (with both Lorentz and Voigt line shapes), the narrow-band model (with Curtis-Godson scaling), and the broadband model (with Chan-Tien scaling), are summarized in Table 3. These refer to the column labeled "nonhomogeneous." Note that line-by-line calculations do not necessitate use of scaling approximations. But the differences in the tabulated nonhomogeneous band absorptances contain not only differences due to scaling approximations, but also differences which exist between the line-by-line, narrow-band and broadband models. To factor out this latter effect, we have also evaluated the band absorptance for an equivalent homogeneous column and then ratioed the nonhomogeneous to homogeneous band absorptances. In this way, errors due to scaling approximations are largely isolated through comparison of the ratios. The results of Table 3 indicate that, at least for tropospheric conditions, the narrow-band and broadband scaling approximations are quite adequate.

Similar comparisons are given in Table 4 for the stratospheric column (13–50 km). Here the error is referenced to the line-by-line calculation for Lorentz lines, since this is the line shape inherent within the two band models. But note that use of a Voigt versus Lorentz line shape has little significance. The important point is that broadband scaling produces a significantly greater error for the stratospheric column as opposed to the tropospheric column (Table 3).

A subsequent degradation of both scaling procedures occurs when the stratosphere and troposphere are combined; this is evident from the results summarized in Table 5. As originally noted by *Curtis* [1952], scaling approximations are likely to be the least satisfactory for a combination of large amounts of gas at low pressure with small amounts at high pressure, as is the case for ozone. To be more specific on this point, we have additionally considered a hypothetical case in which O_3 is uniformly mixed throughout the atmosphere (Table 6). Here the applicability of the scaling approximations is quite good and is comparable to the uniformly mixed CH_4 results of *Cess et al.* [1986].

A final point concerns the fact the broadband scaling produces a much greater error than does narrow-band scaling (Table 5), and there is a simple explanation for this. Since Curtis-Godson scaling is exact in both the strong- and weak-line limits, then errors associated with this scaling would occur only for conditions removed from either of these two limits. While this might be the case on the average throughout a band, many of the narrow-band spectral intervals could individually be close to either of the two limits, thus minimizing potential errors induced by Curtis-Godson scaling. For the 9.6-μm O_3 band this is indeed the case. For conditions corresponding to Table 5, the central portion of the band is close to

TABLE 5. Comparison of Atmospheric (0–50 km) O_3 Total Band Absorptances for the 9.6-μm Band

Model	Band Absorptance, cm^{-1}		Ratio	Error, %
	Homogeneous	Nonhomogeneous		
Line-by-line (Voigt)	52.66	40.30	0.765	···
Line-by-line (Lorentz)	52.66	40.08	0.761	···
Narrow band	52.56	43.00	0.818	7.5
Broadband	47.06	44.34	0.942	23.1

The homogeneous atmosphere (P = 0.514 atm and T = 263 K) contains the same O_3 amount (0.2943 cm atm) as the nonhomogeneous atmosphere.

TABLE 6. Comparison of Atmospheric (0–50 km) O_3 Total Band Absorptances for the 9.6-μm Band and for the Hypothetical Case of Constant O_3 Mixing Ratio (0.379 ppmv)

Model	Band Absorptance, cm^{-1}		Ratio	Error, %
	Homogeneous	Nonhomogeneous		
Line-by-line	52.66	51.92	0.986	...
Narrow Band	52.56	51.13	0.973	1.3
Broadband	47.06	47.87	1.017	3.1

No distinction is made between use of the Lorentz or Voigt line shapes in the line-by-line calculation, since here the results are the same.

the strong-line limit, while the band wings are in the weak-line limit. Thus errors induced by Curtis-Godson scaling are due solely to the transition from one limit to the other.

With respect to the broadband model, scaling of the line-broadening pressure is comparable to Curtis-Godson scaling. But the significant difference is that here it is averaged over the entire band. Thus instead of departures from either the weak- or strong-line limits being restricted to the aforementioned narrow-band transition region, in broadband scaling this is a band-averaged departure that in turn produces larger errors associated with broadband scaling.

It should be cautioned, however, that this interpretation of scaling errors refers solely to the band absorptance for the total atmospheric column. In section 4 it is demonstrated that such an interpretation is more subtle with respect to flux calculations.

4. Atmospheric Flux Calculations

To facilitate a more meaningful intercomparison of atmospheric radiation models, we consider the effect of O_3 upon the net infrared flux at the surface, at the tropopause (13 km), and at the top of the atmosphere (50 km). The mid-latitude summer atmosphere of section 3 is adopted, again ignoring overlap with water vapor, CO_2, and clouds. These flux computations are as described by *Cess et al.* [1986].

Flux reductions due to the present atmospheric abundance of O_3 are summarized in Table 7. Note first that the choice of Voigt versus Lorentz line shape has virtually no impact upon the line-by-line results, a conclusion at variance with *Morcrette and Fouquart* [1985]. They employed the narrow-band model of *Fels* [1979] that incorporates the Voigt line shape, reverting to the Malkmus model in the absence of Doppler broadening, and they show substantial flux differences for Voigt versus Lorentz line shapes. For example, employing the *McClatchey et al.* [1971] tropical atmosphere, they find that the Voigt line shape, relative to Lorentz, diminishes the flux reduction at the top of the atmosphere by 3.1 W m^{-2}. This is in contrast to our 0.02 W m^{-2} value for the mid-latitude summer atmosphere (Table 7). More recently, however, J. T. Kiehl (private communication, 1987) has repeated the narrow-band calculations of Morcrette and Fouquart and finds the Voigt-Lorentz differences to be negligible, a conclusion which is indeed consistent with our line-by-line calculations.

Next, comparison of the narrow-band model to the line-by-line results (Table 7) shows that the narrow-band model produces a 7% overestimate at the surface and a 9% overestimate at the top of the atmosphere, and these differences are largely attributable to Curtis-Godson scaling. For example, as in section 3, we have separately considered tropospheric and stratospheric O_3 (Table 8). Here as in Table 7, there is virtually no difference between use of the Voigt or Lorentz line shapes, so only the Voigt results are given in Table 8. Both the modest negative errors for the troposphere and the somewhat greater positive errors for the stratosphere are consistent with our prior interpretation of errors associated with Curtis-Godson scaling through use of the column band absorptance (Tables 3 and 4). Then, as in Table 5, larger errors at both the top of the atmosphere and at the surface occur for combined stratospheric and tropospheric O_3 (Table 7). Note also, that the close agreement at the tropopause (Table 7) is actually a consequence of modest compensating errors (Table 8).

The situation is not as straightforward with respect to the broadband model, since here differences relative to the line-by-line results are the collective consequence of errors due to broadband scaling as well as to the aforementioned errors inherent within the band model itself, and it is not possible to separate these effects. Note, however, that while the broadband model is closer to the line-by-line value than is the narrow-band model, at the top of the atmosphere this presumably is due to compensating differences, since the broadband model produces the greatest error at the top of the atmosphere when tropospheric O_3 is removed (Table 8). For comparative purposes we have also included within Table 7 results

TABLE 7. Comparison of Model Calculations for the Reduction in Infrared Flux Due to the Presence of the 9.6-μm Band of O_3

Model	Flux Reduction, W m^{-2}		
	Top	Tropopause	Surface
Line-by-line (Voigt)	9.12	5.84	4.73
Line-by-line (Lorentz)	9.14	5.83	4.72
Narrow band	10.00	5.82	5.05
Broadband	9.82	5.38	4.58
Broadband [*Ramanathan and Dickinson*, 1979]	9.81	5.12	4.48

TABLE 8. Comparison of Model Calculations for the Reduction in Infrared Flux Due to the Presence of the 9.6-μm Band of O_3 Separately Contained Within the Troposphere (0–13 km) and the Stratosphere (13–50 km)

Model	Flux Reduction, W m^{-2}		
	Top	Tropopause	Surface
	0-13 km		
Line-by-line	···	3.70	3.39
Narrowband	···	3.56	3.35
Broadband	···	3.26	3.02
	13–50 km		
Line-by-line	8.08	2.14	···
Narrowband	8.64	2.25	···
Broadband	8.88	2.13	···

employing the broadband model of *Ramanathan and Dickinson* [1979].

We have further performed the standard ICRCCM perturbation in O_3 abundance, consisting of a 25% reduction in stratospheric O_3 and a 25% increase in tropospheric O_3. These results are summarized in Table 9. In contrast to Table 7, for which the maximum broadband error is 8%, in Table 9 it is 15%. Furthermore, for completeness we have performed both present O_3 and perturbed O_3 computations for the 14-μm band, and these are summarized in Tables 10 and 11.

As we have discussed earlier, there is a typographical error in the *McClatchey et al.* [1971] mid-latitude summer atmosphere, and we have retained the uncorrected version. But this error does not substantially impact the flux computations. For example, we have repeated the line-by-line (Voigt) computations of Table 7 employing the corrected mid-latitude summer atmosphere, from which the respective top, tropopause, and surface flux reductions are 9.01, 5.73 and 4.64 W m^{-2}. The results in the top row of Table 7 differ by less than 2% from these values.

On a final point, our Voigt line-by-line results for the combined 9.6- and 14-μm flux reductions (Tables 7 and 10) at the top of the atmosphere, the tropopause, and the surface are, 11.53, 7.38, and 6.31 W m^{-2}, respectively, and these are in excellent agreement with an independent line-by-line calculation (S. B. Fels and M. D. Schwarzkopf, private communication, 1987) that produced the respective values of 11.71, 7.40, and 6.37 W m^{-2}. The modest disagreement at the top of the atmosphere is, in fact, consistent with our use of 50 km for the top of the atmosphere, while Fels and Schwarzkopf employed 70 km. Since both calculations utilize the same AFGL tape, this of course simply indicates that the numerical techniques are mutually consistent.

TABLE 9. Comparison of Model Calculations for the Change in Infrared Flux Due to the 9.6-μm O_3 Band, as Caused by a Change in O_3 Abundance

Model	Flux Change, W m^{-2}		
	Top	Tropopause	Surface
	25% Reduction in Stratosphere O_3		
Line-by-line	0.75	0.23	0.18
Narrow band	0.73	0.24	0.18
Broadband	0.77	0.24	0.21
	25% Increase in Tropospheric O_3		
Line-by-line	−0.22	−0.65	0.52
Narrow band	−0.28	−0.62	0.51
Broadband	−0.21	−0.55	0.44

5. ATMOSPHERIC COOLING RATES

We now briefly turn to a comparison of cooling rates as predicted by the respective band models, again employing the *McClatchey et al.* [1971] mid-latitude summer atmosphere. This comparison is given in Figure 3 for the 9.6-μm band, and we note that truncation of the atmosphere at 50 km produces artificially large cooling rates near the top of the model atmosphere, due to the absence of downward emission from levels above 50 km. But the point here is to provide a band model comparison. Note from the line-by-line calculations that use of the Lorentz line shape is quite adequate below roughly 40 km, as is consistent with earlier studies [*Ramanathan*, 1976; *Ramanathan and Coakley*, 1978; *Fels*, 1979].

With reference to the applicability of Curtis-Godson scaling to cooling rate computations, this has been addressed by *Ramanathan and Coakley* [1978] using a modification of the Malkmus model [*Rodgers*, 1968] that avoids use of scaling approximations through assuming that all lines within a given spectral interval are replaced by a single effective line. Conversely, as in section 4, the near-precise agreement between the narrow-band and line-by-line models, for homogeneous paths, allows an alternate means of testing Curtis-Godson scaling. The narrow-band versus line-by-line comparison in Figure 3 below 40 km, where pressure broadening dominates, is consistent with the conclusion of *Ramanathan and Coakley* [1978] that Curtis-Godson scaling produces a modest underestimate in stratospheric cooling rate. This is less than 0.2 K day^{-1} and, as Ramanathan and Coakley point out, is a small error relative to the roughly 5 day^{-1} cooling due to all atmospheric constituents. The somewhat greater underestimate associated with the broadband model is consistent with flux differences discussed in the previous section.

As a final point, we return to the uncorrected versus corrected McClatchey et al. mid-latitude summer atmosphere. The difference in cooling rate, as determined from line-by-line (Voigt) calculations, is illustrated in Figure 4. As expected, the differences are restricted to those altitudes where the uncorrected model atmosphere overestimates the ozone abundance.

6. CONCLUDING REMARKS

The present study shows that for a homogeneous column of ozone, the narrow-band model of *Malkmus* [1967] produces total band absorptances that are in near-precise agreement

TABLE 10. Comparison of Model Calculations for the Reduction in Infrared Flux Due to the Presence of the 14-μm Band of O_3

Model	Flux Reduction, W m^{-2}		
	Top	Tropopause	Surface
Line-by-line (Voigt)	2.41	1.54	1.58
Line-by-line (Lorentz)	2.40	1.54	1.57
Narrow band	2.48	1.50	1.68
Broadband	2.62	1.37	1.48

TABLE 11. Comparison of Model Calculations for the Change in Infrared Flux Due to the 14-μm O_3 Band, as Caused by a Change in O_3 Abundance

Model	Flux Change, W m^{-2}		
	Top	Tropopause	Surface
25% Reduction in Stratospheric O_3			
Line-by-line	0.43	0.24	0.24
Narrow band	0.44	0.24	0.26
Broadband	0.51	0.25	0.25
25% Increase in Tropospheric O_3			
Line-by-line	−0.06	−0.08	−0.09
Narrow band	−0.09	−0.07	−0.10
Broadband	−0.08	−0.07	−0.09

with line-by-line calculations, a conclusion that should not be extended to other gases [e.g., *Cess et al.*, 1986]. Thus when applied to atmospheric radiation calculations, differences between the Malkmus and line-by-line models are primarily attributable to errors induced through use of Curtis-Godson scaling in conjunction with the narrow-band model.

For flux calculations this typically leads to errors of roughly 10% or less, in contrast to methane [*Cess et al.*, 1986], for which errors due to Curtis-Godson scaling are of the order of 1% or less. This difference in behavior between O_3 and CH_4 is shown to be a consequence of the combination of large amounts of O_3 at low pressures with small amounts at high pressures. *Curtis* [1952] originally suggested that scaling approximations are likely to be least accurate under these conditions. But for cooling rate calculations, errors due to Curtis-Godson scaling are less than 0.2 K day^{-1}, consistent with *Ramanathan and Coakley* [1978], who employed the narrow-band model of *Rodgers* [1968] that does not necessitate a scaling approximation.

The broadband model produces somewhat greater errors, both with respect to atmospheric fluxes and cooling rates, than does the narrow-band model. This is due to the broadband scaling being less satisfactory than Curtis-Godson scaling, in addition to inherent inaccuracies of the broadband model, despite the fact that this model has been tuned to the line-by-line model.

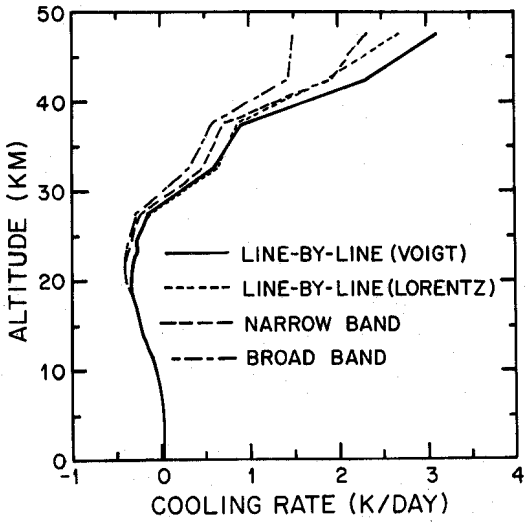

Fig. 3. Cooling rate comparisons for the 9.6-μm ozone band.

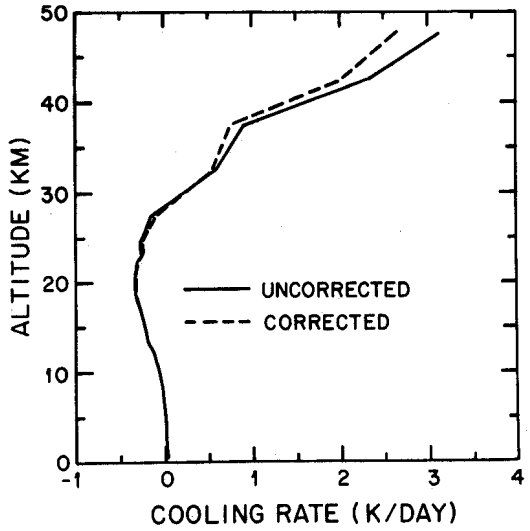

Fig. 4. Cooling rate comparison for the uncorrected and corrected *McClatchey et al.* [1971] mid-latitude summer atmosphere.

While the line-by-line calculations show that Doppler broadening impacts cooling rates above roughly 40 km, as is consistent with other studies [*Ramanathan*, 1976; *Ramanathan and Coakley*, 1978; *Fels*, 1979], this has a negligible effect upon atmospheric flux calculations.

Acknowledgments. We benefited from useful discussions with S. B. Fels and J. T. Kiehl. This work was supported by the National Science Foundation through Grant ATM8515310.

REFERENCES

Aida, M., A theoretical examination of absorption in the 9.6 micron ozone band, *J. Quant. Spectrosc. Radiat. Transfer, 15*, 389–403, 1975.

Cess, R. D., and V. Ramanathan, Radiative transfer within the atmosphere of Mars and that of Venus above the cloud deck, *J. Quant. Spectrosc. Radiat. Transfer, 12*, 933–945, 1972.

Cess, R. D., and L. S. Wang, A band absorptance formulation for nonisothermal gaseous radiation, *Int. J. Heat Mass Transfer, 13*, 547–555, 1970.

Cess, R. D., D. P. Kratz, S. J. Kim, and J. Caldwell, Infrared radiation models for atmospheric methane, *J. Geophys. Res., 91*, 9857–9864, 1986.

Chan, S. H., and C. L. Tien, Total band absorptances of nonisothermal infrared-radiating gases, *J. Quant. Spectrosc. Radiat. Transfer, 9*, 1261–1271, 1969.

Curtis, A. R., A discussion of "A statistical model for water vapor absorption," *Q. J. R. Meteorol. Soc., 78*, 638–640, 1952.

Edwards, D. K., and S. J. Morizumi, Scaling of vibration-rotation band parameters for nonhomogeneous gas radiation, *J. Quant. Spectrosc. Radiat. Transfer, 10*, 175–188, 1970.

Fels, S. B., Simple strategies for inclusion of Voigt effects in infrared cooling rate calculations, *Appl. Opt., 18*, 2634–2637, 1979.

Goody, R. M., A statistical model for water vapor absorption, *Q. J. R. Meteorol. Soc., 78*, 165–169, 1952.

Kiehl, J. T., and V. Ramanathan, CO_2 radiative parameterizations used in climate models: Comparison with narrow-band models and with laboratory data, *J. Geophys. Res., 88*, 5191–5202, 1983.

Kuriyan, J. G., Z. Shippony, and S. B. Mitra, Transmission function for infrared radiative transfer in an inhomogeneous atmosphere, *Q. J. R. Meteorol. Soc., 103*, 55–517, 1977.

Luther, F. M., and Y. Fouquart, The intercomparison of radiation codes in climate models (ICRCCM), *WMO Rep. WCP-93*, 37 pp., World Meteorol. Organ., Geneva, Switzerland, 1984.

Malkmus, W., Random Lorentz band model with exponential tailed S^{-1} line-intensity distribution function, *J. Opt. Soc. Am., 57*, 323–329, 1967.

McClatchey, R. A., R. W. Fenn, J. E. A. Selby, F. E. Volz, and J. S. Garing, Optical properties of the atmosphere, *Rep. AFCRL-71-*

0279, 85 pp., Air Force Cambridge Res. Lab., Cambridge, Mass., 1971.

Morcrette, J.-J., and Y. Fouquart, On systematic errors in parameterized calculations of longwave radiation transfer, *Q. J. R. Meteorol. Soc.*, *111*, 691–708, 1985.

Ramanathan, V., Radiative transfer within the Earth's troposphere and stratosphere: A simplified radiative-convective model, *J. Atmos. Sci.*, *33*, 1330–1346, 1976.

Ramanathan, V., and J. A. Coakley, Jr., Climate modeling through radiative-convective models, *Rev. Geophys.*, *16*, 465–489, 1978.

Ramanathan, V., and R. E. Dickinson, The role of stratospheric ozone in the zonal and seasonal radiative energy balance of the Earth-troposphere system, *J. Atmos. Sci.*, *36*, 1084–1104, 1979.

Rodgers, C. D., Some extensions and applications of the new random band model for molecular band transmission, *Q. J. R. Meteorol. Soc.*, *94*, 99–102, 1968.

Rodgers, C. D., and C. D. Walshaw, The computation of infrared cooling rate in planetary atmospheres, *Q. J. R. Meteorol. Soc.*, *92*, 67–92, 1966.

Rothman, L. S., R. R. Gamache, A. Barbe, A. Goldman, J. R. Gillis, L. R. Brown, R. A. Toth, J. M. Flaud, and C. Camy-Peyret, AFGL atmospheric absorption line parameters compilation: 1982 edition, *Appl. Opt.*, *22*, 2247–2256, 1983.

Yamamoto, G., M. Aida, and S. Yamamoto, Improved Curtis-Godson approximation in a non-homogeneous atmosphere, *J. Atmos. Sci.*, *29*, 1150–1155, 1972.

R. D. Cess, Laboratory for Planetary Atmospheres Research, State University of New York at Stony Brook, Stony Brook, NY 11794.

D. P. Kratz, Code 613, NASA Goddard Space Flight Center, Greenbelt, MD 20771.

(Received October 13, 1987;
revised February 22, 1988;
accepted March 8, 1988.)